Influence of 20-hydroxyecdysone on skeletal muscle inflammation following eccentric damage

by

William Luke Johnson IV

Honors Thesis
Appalachian State University

Submitted to The Honors College
in partial fulfillment of the requirements for the degree of

Bachelor of Science

May, 2018

Approved by:

Kevin A. Zwetsloot, Ph.D., Thesis Director

Jennifer P. Cecile, Ph.D., Second Reader

Jefford Vahlbusch, Ph.D., Dean, The Honors College

ABSTRACT

Inflammation plays an important role in the skeletal muscle repair process after damage. In addition to exerting anabolic/growth effects on skeletal muscle, phytoecdysteroids, like 20-hydroxyecdysone (20E), have been reported to possess anti-inflammatory properties. The purpose of this study was to investigate the influence of 20E on the inflammatory response to eccentric damage in mouse skeletal muscle. Male mice (3-6 months of age) were (DHR) or were not (No DHR) subjected to eccentric damage via an acute bout of downhill running to exhaustion. Mice were treated daily with 20E (50mg/kg body mass) or vehicle for two or five days, and sacrificed on the next day. Using immunohistochemical techniques, expression of interleukin-6 (IL-6) and monocyte chemoattractant protein-1 (MCP-1) were examined in fresh-frozen gastrocnemius muscles. From a semi-quantitative analysis, treatment of 20E was seen to reduce expression of IL-6 and MCP-1 following an acute bout of DHR; which indicates that 20E may exhibit anti-inflammatory activity in response to skeletal muscle damage. These results, previous work in our lab, and the overwhelming amount of literature showing anabolic effects of 20E, suggest that there may be a novel mechanism allowing both catabolic and anabolic steroid-like activity.

Acknowledgements

I would like to thank both the Office of Student Research and the Honors College for funding, as well as Department of Health & Exercise Science for the invaluable resources offered.

Dedication

To my thesis director, Dr. Kevin A. Zwetsloot, thank you for the generous support you have given me over the past few years as an advisor and friend. Working in your lab has truly been a great experience. I have learned a lot more than I would have ever imagined; without the research experience in your lab I would definitely not have such a great appreciation for high quality, immunohistochemically prepared, fluorescent images. You are a great mentor who I look forward to seeking advice from as a researcher, and a friend in the future.

To everyone in the Integrative Muscle Physiology Lab, thank you for the help and support. This project would not have been possible without the help of many people for everything from caring for, and treating the mice, to harvesting and preparing the tissue samples. I will always cherish the friendships that were made when working in the lab early in the morning and late at night. I would also like to thank my second reader, Dr. Jennifer P. Cecile, for being so supportive and flexible, as things changed and dates moved.

Lastly, I would like to thank my family members and close friends. There were many times when I was upset with how everything was going, and during those moments, I truly appreciate the time you took to listen, and offer words of encouragement. I would especially like to thank my parents, Pam and Bill Johnson, for the support you have unconditionally provided. It was your support that played a large role in the process of becoming who I am today, and ultimately keeping the motivation alive throughout this long grueling process.

Table of Contents

Abstract……..……1

Acknowledgments……..…2

Dedication……..….3

Introduction……..…...5

Methods……..……11

Results……..…..15

Discussion……..…..…21

References……..25

Vita……27

INTRODUCTION

Skeletal muscle damage

Movement is not possible without the contraction of skeletal muscle, which occurs when sarcomeres shorten as a result of actin and myosin cross bridge cycling (Douglas, et al., 2017). Depending on the relationship between the magnitude of the contractile force and the load on the muscle, three different types of contraction can occur; eccentric, isometric, or concentric. Eccentric contractions occur when the contractile force is less than the load force, producing a lengthening of the muscle as it contracts (Douglas, et al., 2017) (Marqueste, et al., 2008). It is thought that the forceful lengthening in an eccentric motion induces damage by forcibly detaching myosin protein heads from actin (Douglas, et al., 2017) (Marqueste, et al., 2008) (Hody, et al., 2013). Because of this, eccentric movement has been used to induce muscle damage in a research setting. One common method for this in rodents is downhill running (DHR), which induces damage to muscles of the hind limbs. Eccentric damage from DHR is most apparent in muscles attached to multiple joints, such as the gastrocnemius (Hody, et al., 2013).

Inflammatory processes in skeletal muscle repair

After damage occurs in a muscle, the body must repair it; this highly regulated process can be credited to the work of leukocytes, specifically mononucleated myeloid cells, invading the sites of damage. Of the invading inflammatory cell populations, neutrophils and macrophages are the most abundant. Neutrophils arrive first, invading the damaged tissue within an hour of injury (Tidball, 2005). During the acute inflammatory phase, these cells release pro-inflammatory cytokines such as IL-6 and tumor necrosis factor-α (TNF- α) , as well as myeloperoxidase (MPO) and free radicals. MPO and free radicals are responsible for the

oxidative activity and identification of damaged muscle fibers for phagocytosis by subsequent inflammatory cells (Tidball, et al., 2010) (Tidball, 2005). Concentrations of neutrophils and their respective cellular activity can be affected by many factors. Intensity of exercise and the environmental conditions in the tissue have been shown to alter protein expression and population size in neutrophilic cells (Tidball, 2005) (Pierre-Schneider, et al., 2007). In addition to secretion of cytokines and other products, neutrophils also exhibit phagocytic activity, removing early necrotic cellular debris found in damaged tissue (Tidball, 2005) (Reid, et al., 1992).

Before monocytes can repair damaged tissue, they must be signaled to infiltrate the damaged area; this is done in part largely through the secretion of inflammatory cytokines and chemokines. The signaling event begins at the onset of the injury, when type 1 mature T helper cells (Th1) release Th1-derived cytokines, such as interleukin 6 (IL-6) and interleukin 10 (IL-10) (Tidball, et al., 2010) (Tidball, 2005). Of the infiltrating macrophages, there are two distinct phenotypes, which function in vastly different ways. M1 macrophages, identified by expression of $CD68^{+}$, are activated and signaled to the site of damage by Th1 cytokines. M1 macrophages are thought to perpetuate inflammation further by producing pro-inflammatory cytokines such as IL-6 and TNF- α, as well as cytotoxic levels of nitric oxide (Tidball, 2005). These leukocytes exhibit phagocytic activity on the cellular debris in the injured tissue. The decline in M1 macrophages occurs after the phagocytic stage of repair, which is often two to four days after the injury (Tidball, 2005).

During the decline of the M1 macrophages, cell populations of M2 macrophages begin to rise as the tissue transitions into a more regenerative state. The M2 macrophages can be divided into three smaller sub-species, M2a, M2b, and M2c (Nielsen, et al., 2007) (Tidball, 2005). Initiated by Th2 derived cytokines Interleukin-3 (IL-3) and Interleukin-4 (IL-4), M2a

macrophages correspond to the end of the phagocytic stage, as they inhibit NO-mediated lysis by the M1 macrophages. Muscle fibrosis is also promoted by M2a macrophages through the metabolism of arginine by arginase (Nielsen, et al., 2007) (Liping, et al., 2009). M2b macrophages are activated by immune complexes such as CD32, which results in the release of anti-inflammatory Th2 cytokines. Activated by interleukin-10 (IL-10), M2c cells release cytokines such as IL-1, IL-4, and IL-10, which serve to further deactivate M1 macrophages and stimulate fibroblast proliferation (Tidball, et al., 2010) (Tidball, et al., 2007). Ultimately, the activity of the neutrophils and macrophages results in injured tissue returning to a 'healthy' state.

Interleukin-6 (IL-6)

IL-6 has been shown to have a plethora of both anti-inflammatory and pro-inflammatory effects. In skeletal muscle, IL-6 is primarily defined by its pro-inflammatory activity, as IL-6 deficient mice produce a compromised acute inflammatory response after tissue damage (Munoz-Canoves, et al., 2013). Muscle damage can also induce hypertrophy, or the increase in skeletal muscle fiber size or cross-sectional area, as a result of the repair process. Hypertrophy requires increased protein synthesis, as well as the growth of new nuclei from the progeny of satellite cells. In IL-6 knockout mice, hypertrophy of myofibers is impaired as a result of inadequate accumulation of new nuclei, which supports that IL-6 plays an important role in regulating the activity of satellite cells (Serrano, et al., 2008). Several studies have shown that expression of IL-6 in skeletal muscle is directly related to the magnitude of damage incurred on the tissue (Bruunsgard, et al., 1997) (Nielsen, et al., 2007).

IL-6 stimulates cells through two signaling pathways: classical signaling and trans-signaling. During classical signaling, IL-6 becomes bound to IL-6 receptor protein, which can then associate with the signaling protein gp130 found on the same cell (Munoz-Canoves, et al., 2013) (Nielsen, et al., 2007). Activation of gp130 leads to dimerization, then activation of Janus kinases (JAK); which results in phosphorylation of tyrosine residues on gp130 (Munoz-Canoves, et al., 2013). This phosphorylating event ultimately results in activation of the ras/raf/mitogen-activated protein (MAP) kinase pathway, which activates various transcriptional factors for growth and signal transduction. Cells lacking the IL-6 receptor cannot be activated by this cytokine directly. However they can be activated via trans-signaling, when a soluble form of the IL-6 receptor protein, bound to IL-6, associates with gp130. Trans-signaling activation results in primarily pro-inflammatory events, while classic IL-6 signaling results in regenerative and anti-inflammatory events (Munoz-Canoves, et al., 2013).

Monocyte chemoattractant protein-1 (MCP-1)

Attracted to the site of injury by monocyte chemoattractant protein-1 (MCP-1), macrophages begin to infiltrate the tissue 24 hours after injury. MCP-1 is a necessary chemokine secreted by skeletal muscle for successful regeneration (Tidball, 2005). MCP-1 is unique from many chemokines in that it is specific to the signaling of only macrophages, and without it present in the tissue, both infiltration of macrophages and repair/regeneration is significantly reduced (Tidball, et al., 2007).

Phytoecdysteroids

Composed of a polyhydroxylated ketosteroid structure, ecdysteroids are signaling hormones found in insects to trigger molting. Some species of plants produce similar compounds, known as phytoecdysteroids, which are similar in structure and are thought to act as a defense mechanism against invading insects by inducing molting, which, if premature, will result in insect death (Gorelick-Feldman, et al., 2010). Phytoecdysteroids have similar structural elements to vertebrate steroid hormones, making them a class of anabolic steroids which can induce some similar effects, such as lowering cholesterol and blood glucose levels, anabolic growth, and immunomodulation (Lafont, et al., 2003). While these compounds can induce anabolic effects, they do not bind to an androgen receptor, therefore phytoecdysteroids do not result in negative androgenic responses (e.g. rapid growth of all tissues). Rather than binding to a canonical intracellular androgen receptor, their proposed mechanism of action is thought to involve a cell surface membrane bound G-protein receptor (Gorelick-Feldman, et al., 2010).

After injury, anabolic steroids, such as nandrolone decanoate, cause a greater inflammatory response which results in reduced strength during the early phagocytic stage, but then a greater strength after fully healed when compared to a control. Corticosteroids on the other hand, inhibit protein synthesis and have anti-inflammatory abilities, reducing the inflammatory response, which results in a greater strength in early stages of recovery, but then a reduced strength after being fully healed when compared to a control (Beiner, et al., 1999).

20-hydroxyecdysone (20E), a common phytoecdysteroid produced by spinach, has been shown to activate the Akt/mTOR pathway in mice, increase grip strength in mice, and increase protein synthesis in cultured skeletal muscle cells (Gorelick-Feldman, et al., 2010) (Gorelick-Feldman, et al., 2008). Work from late Soviet Union reported that 20E evokes anti-inflammatory effects in skeletal muscle repair (Kurmukov, et al., 1988).

This anti-inflammatory ability is intriguing, since 20E can also induce anabolic-like effects of increasing protein synthesis, which would traditionally be thought of as the opposite of anti-inflammatory. Outside of the original Soviet research, very little is known about how 20E might affect the acute inflammatory response in skeletal muscle cells. Our lab previously reported that 28 days of 20E supplementation induces hypertrophy (increased fiber cross-sectional area) and stimulates protein synthesis signaling in muscle of aged mice (unpublished data). On the contrary, we have demonstrated that 20E supplementation does not have the same effect on skeletal muscle of young mice (unpublished data). Therefore, we have progressed to investigating whether 20E supplementation augments the repair of skeletal muscle after damage.

Purpose and Hypotheses

The purpose of this study was to investigate if 20E influences the inflammatory response in skeletal muscle after an acute bout of downhill running (DHR). Based on previous literature on steroids and muscle damage, I hypothesized that the administration of 20E would result in a larger inflammatory response early on, shown as a greater expression of IL-6 and MCP-1 two days post-injury. I also hypothesized that 20E would result in quicker recovery, seen at five days post-injury as less expression of IL-6 and MCP-1 with 20E treatment than with vehicle treatment.

METHODS

Mouse Model

All procedures in this study were approved by the Institutional Animal Care and Use Committee at Appalachian State University. Maintained on a reverse 12-hour light and 12-hour dark cycle, 3-6 month old male C57BL/6 mice were assigned to 8 groups, 4 control groups (no DHR) and 4 DHR groups. The breakdown of various treatment groups is shown in Figure 1.

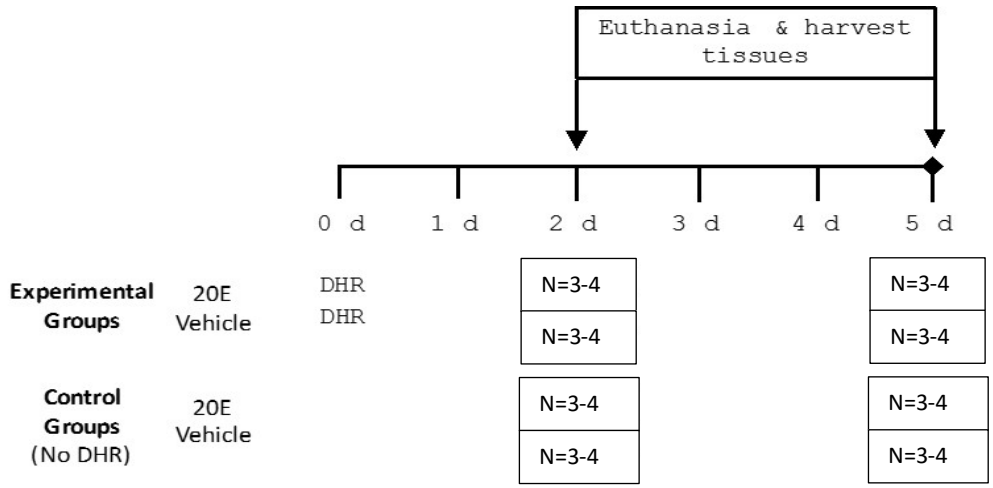

Figure 1. Protocol Schematic of various sample groups

For the DHR groups, mice were acclimated to the rodent treadmill over five consecutive days, going from 0 m/min the first day, to 11m/min the last, with 0° decline throughout. On the next day, immediately after the acclimation protocol, the DHR groups performed an acute bout of DHR to exhaustion at 17 m/min with a -20° decline. After completion of the DHR, mice were given a brief period of time to recover before they received an oral gavage treatment of either 50 mg/kg of body mass of 20E dissolved in vehicle (rodent liquid diet, BioServ AIN-76) or vehicle only, and then returned to their cage. In the cage, mice had ad libitum access to chow and water. For the next one (2-day treatment groups) or four (5-day treatment groups) consecutive days, mice were given the same gavage treatment, and weighed daily to monitor health. This gavage treatment protocol was replicated for the four control (no DHR) groups, with either 20E in

vehicle (20E), or vehicle alone (vehicle). Mice were anesthetized with 4% isoflorane inhalation, and euthanized via cervical dislocation.

Tissue Harvest and Preparation

The left gastrocnemius muscle was dissected and mounted to cork using a paste of tragacanth gum and mounting media (TissueTek, O.C.T.), then liberally coated in mounting media before being frozen in liquid isopentane. All samples were stored either on dry ice during transport, or in a freezer at -80°C. Tissues were sectioned at -18°C using a cryostat (Thermo Scientific, Cryostar NX50). Five slides, each containing 6 - 10μm thick sections, were prepared from each tissue sample.

Tissue Staining

Using one slide from each tissue, samples were stained using a hematoxylin and eosin (H&E) staining protocol (Sigma Aldrich, Inc.). From the H&E analysis, the samples which were deemed to be unusable due to freeze fracture were omitted from later immunohistochemical analysis. Using gastrocnemius samples (n=3-4 per group) for the fluorescent identification of IL-6 and MCP-1, samples were first allowed to warm up to room temperature, the O.C.T. was removed, and tissues were then encircled using a hydrophobic-barrier PAP pen (Vector, ImmEdge pen). Samples were blocked by incubating with approximately 75μL of 10% normal goat serum (Vector, S-1000) in 1X phosphate buffered saline (PBS) containing 0.04% triton X-100. Samples were then incubated overnight (12-16 hrs) with a primary antibody cocktail. The 3 sections on the left of each slide received a cocktail of: 1:100 rat, anti-mouse IL-6 specific antibody (Novus, NBP1- 66603) and 1:200 laminin antibody, conjugated to an AlexaFlour (AF) 547 fluorophore (Novus NBP1-75380). Following primary antibody incubation, samples were

washed for 3x5 minutes with approximately 75µL of 0.04% triton X-100 in 1X PBS (Wash buffer). Next, a secondary antibody solution was prepared with donkey, anti-rat conjugated to AF488 (Novus, NBP 1-75380) at a dilution of 1:250 in the 10% NGS solution, and then incubated on samples for 1 hour in the dark. Afterward, samples were washed again for 3x5 min using the wash buffer. After drying fully, coverslips were applied using Vechashield® Hardset with DAPI (Vector, H-1500).

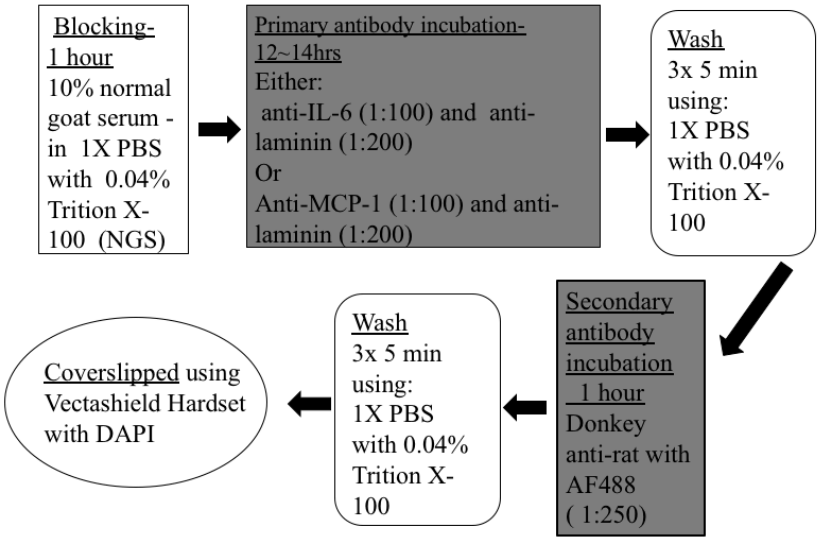

Figure 2. Schematic of IHC Staining Protocol

Microscopy

The samples stained with H &E were imaged under bright field light using a microscope (ThermoFisher Scientific, EVOS FLc) at 4X, 10X, 20X , and 40X magnification. The overall best section on each slide was imaged, primarily looking at possible areas of inflammation under the higher objectives. With the fluorescent-labeled samples, 1-2 clear fields of view at 10X magnification, and 3 fields of view at 20X- coverslip corrected magnification were imaged. For each field of view, an image was captured under the following lamps: DAPI, GFP, and Cy5. Images were then stacked as one complete image. Fields of view were chosen based on the lack of folds/wrinkles present, as well as areas that represented the general average appearance of each sample section. Similar image settings and exposure times were used throughout all imaging to allow for a clearer comparison between samples. Analyzing images representative of

the whole tissue sample, fluorescence was semi-quantitatively determined for the fluorophores bound to the IL-6 and MCP-1 specific antibodies. For each sample, fluorescence was reported in terms of Relative Fluorescence Units (RFUs) , with '0' corresponding to no fluorescence, and '5' corresponding to most fluorescence (Labno, n.d.).

Fluorescence was also analyzed via ImageJ software as well. After opening each image in the program (FIJI, ImageJ), it was split into individual color profiles , producing three separate grey-scale images, corresponding to the stacked red, green, and blue images. The green profile, which corresponded to either IL-6 or MCP-1 bound antibodies, was analyzed for 'Area', 'Mean gray value', and 'Min & max gray value'. To calculate these values, the entire region of the image was encircled using the pencil tool, this allowed strong artifacts to be omitted from the calculation. For the selected region, ImageJ calculated and outputted values for the area, mean intensity, integrated density, and raw integrated density. To determine the intensity and integrated density of the background, a small, totally black area of each image was circled and analyzed. Samples were assigned a number to keep the researcher blinded until after the data were analyzed, where it was then sorted into respective groups and analyzed. The corrected total fluorescence (CTF) was calculated by subtracting the product of 'mean intensity of the background' and 'area of the cell', from the 'integrated density' of the whole image. Variability was reported as the standard deviation for each respective group. Due to small sample sizes, variances in IHC technique, and the large variability between samples, it is difficult to determine the validity of the results from this method. Therefore, the ImageJ analysis will primarily serve to support the results collected from the semi-quantitative analysis of observed fluorescence.

RESULTS

DHR times and Tissue Mass

Of the 2-day treatment groups, the vehicle group DHR run was significantly longer at 78.4 ± 14.5 minutes, than the 20E group at 54.5 ± 7.8 minutes. At the 5-day timepoint, no significant difference in DHR run time was observed between the vehicle and 20E groups; 65.8 ± 15.5 minutes vs. 59.0 ± 7.6 minutes, respectively. At the time of sacrifice, the wet mass of each tissue was recorded. Tissue masses were normalized as a ratio to body mass ($mg_{tissue} \bullet g_{BM^{-1}}$) to analyze for differences between treatment groups. No significant difference was observed at the 2-day (p= 0.410) and 5-day (p= 0.319) time points between 20E and vehicle treatment groups, respectively (Table 1).

Table 1. Ratio of Muscle Tissue Wet Mass to Body Weight ($mg_{tissue} \bullet g_{BM^{-1}}$)

	2-day		5-day	
	No DHR	DHR	No DHR	DHR
Vehicle	4.94 ± 0.19	4.73 ± 0.33	4.76 ± 0.49	4.69 ± 0.24
20E	5.00 ± 0.28	4.72 ± 0.31	4.84 ± 0.38	4.51 ± 0.24
	ANOVA: p= 0.410		ANOVA: p= 0.319	

Morphological Analysis of Muscle Structure

From analysis of the H&E stained gastrocnemius muscle sections, discreet areas composed of distorted fiber structure and extra nuclei were observed for the DHR groups. The acute bout of DHR did produce some areas of minor visual damage in the muscle, however the areas were small in reference to the total cross-sectional size of the gastrocnemius muscle, as well as infrequent across various treatment groups. Images of H&E stained sections can be found in the supplemental material.

Immunohistochemical Analysis of Inflammatory Cytokine Expression

Two inflammatory cytokines were indirectly identified using IL-6 and MCP-1 specific antibodies, paired with a secondary antibody conjugated to a fluorophore. From the 20X magnification images, the most representative one(s) of each sample were analyzed.

Notable in the DHR + vehicle treatment groups, was the difference in expression of inflammatory cytokines in various individual fibers. Fluorescence associated with IL-6 and MCP-1 was chiefly present around the sarcolemma at low levels of fluorescence, as fluorescence increased there was a discrete transition from no fluorescence in a fiber, to consistent fluorescence throughout a fiber. Even in what appeared to be the most injured tissues, fluorescence varied from fiber-to-fiber, greatly, The difference (i.e. heavily abundant in one fiber, but non-existent in the next) was more apparent with MCP-1 than IL-6. Representative images of each group are displayed in Figures 3 and 4, below.

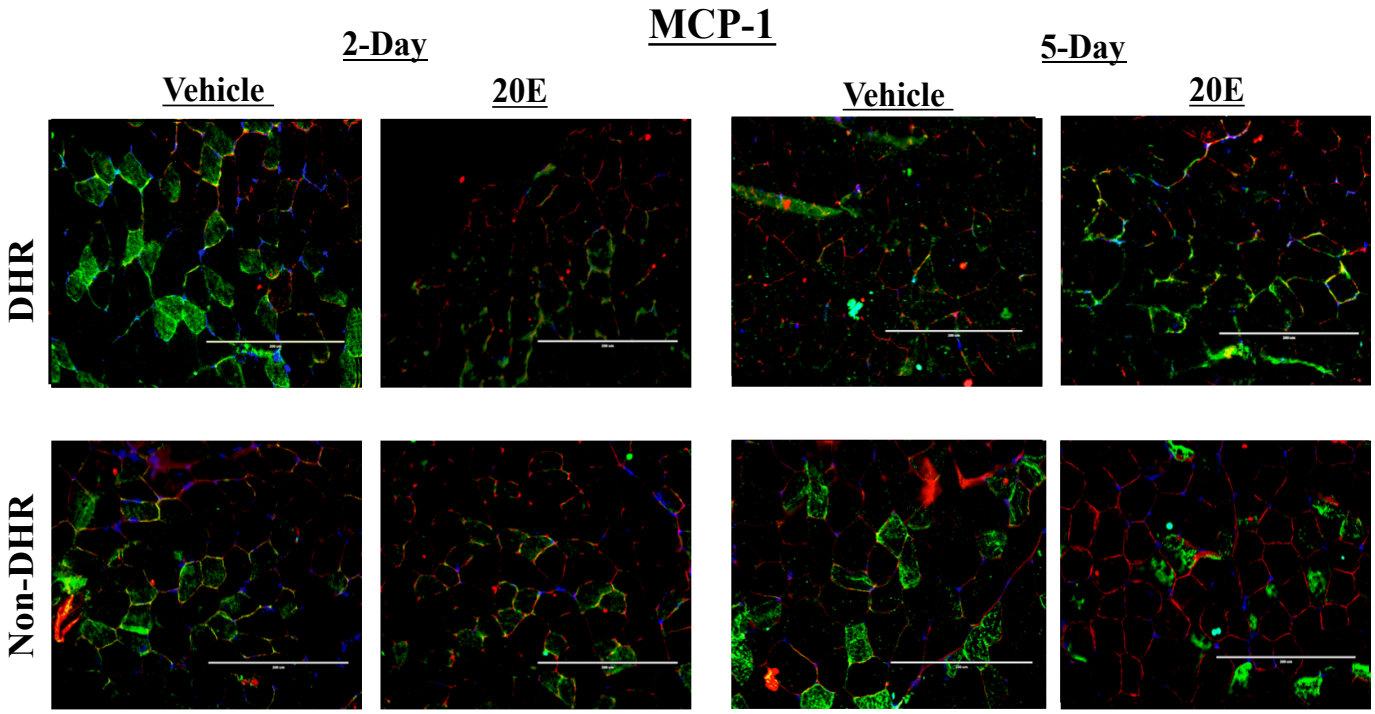

Figure 3. Representative images of MCP-1 expression from gastrocnemius. Green= MCP-1, Red=Laminin (sarcolemma marker) , Blue= DAPI-stained nuclei. Scale Bar= 200µm

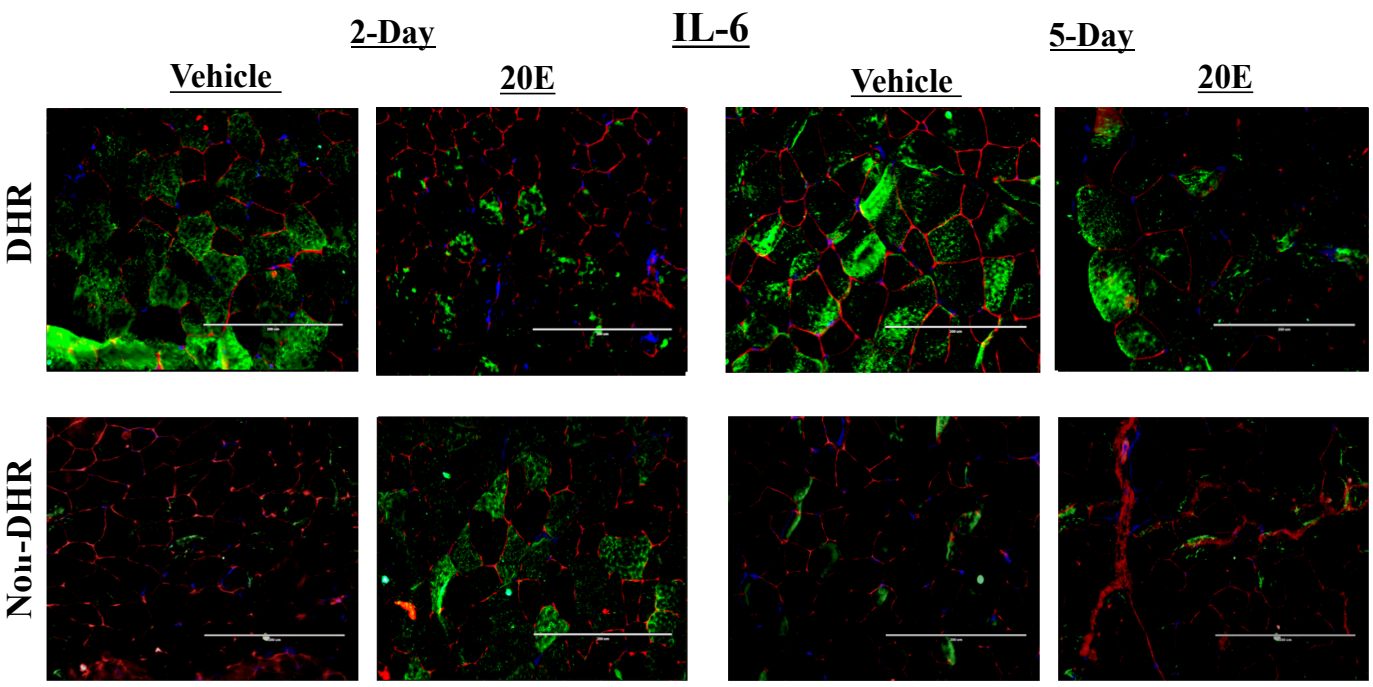

Figure 4. Representative images of MCP-1 expression from gastrocnemius. Green= MCP-1, Red=Laminin (sarcolemma marker) , Blue= DAPI-stained nuclei. Scale Bar= 200µm

Using an arbitrary scale of 0-5 RUFs, with '0' corresponding to no fluorescence and '5' corresponding to the most fluorescence, expression levels of IL-6 and MCP-1 were semi-quantitatively analyzed based on observed fluorescence. For MCP-1, slightly more fluorescence was observed in the 2-day DHR groups, than the 2-day No DHR groups. 2-day treatment of 20E flowing DHR resulted in less fluorescence than vehicle treatment, 1.50 ± 0.5 RFU vs. 2.75 ± 1 RFU. After 5 days of treatment following DHR, fluorescence for MCP-1 has increased to 2 .0± 0.8 RFU with 20E treatment, and 2.80 ± 1 RFU with vehicle treatment. In the 5-day No DHR groups, MCP-1 corresponding fluorescence was similar between 20E and vehicle treatment, at 1.50 ± 1 RFU and 1.83 + 1 RFU respectively. These values in the 5-day No DHR groups reflect an increase over the 2-day No DHR treatment groups, which were reported to be 1.33 ± 0.8 RFU with 20E , and 1.0 ± 0.5 RFU with vehicle. These results are shown in figure 5.

For the antibodies specific to IL-6, 2-day treatment of 20E flowing DHR resulted in fluorescence of 2.16 ± 0.3 RFU; this was observed to be less than the DHR 2-day vehicle treatment, which resulted in 3.5 ± 0.5 RFU. The 2-day DHR treatment groups showed more fluorescence than the 2-day No DHR treatment groups. Compared to 2-day DHR groups, fluorescence for IL-6 specific antibodies was observed to be reduced in both 5-day DHR groups, at 1.8 ± 1 RFU with 20E treatment, and 3.2 ± 0.8 RFU with vehicle treatment. More fluorescence was also determined to be present in the 5-day DHR groups than the 5-day No DHR. Additionally, fluorescence was higher in the 5-day No DHR groups than the 2-day No DHR groups. Observed fluorescence results for IL-6 are shown in figure 6, below.

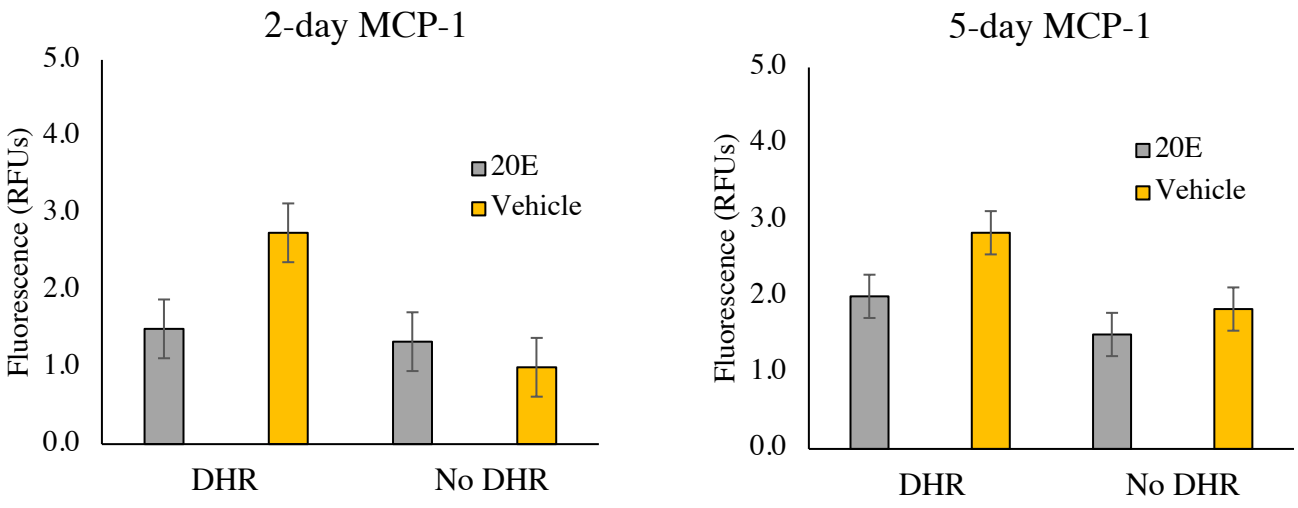

Figure 5. Expression of MCP-1 Determined by Observed Fluorescence Analysis
Expression of MCP-1, quantified in terms of average fluorescence (in RFUs),where 0= no fluorescence and 5= most fluorescence. On the x-axis is treatment groups, arranged by injury (DHR vs. No DHR), with yellow bars representing Vehicle treatment and gray bars representing 20E. Error bars for both graphs reflect standard error.

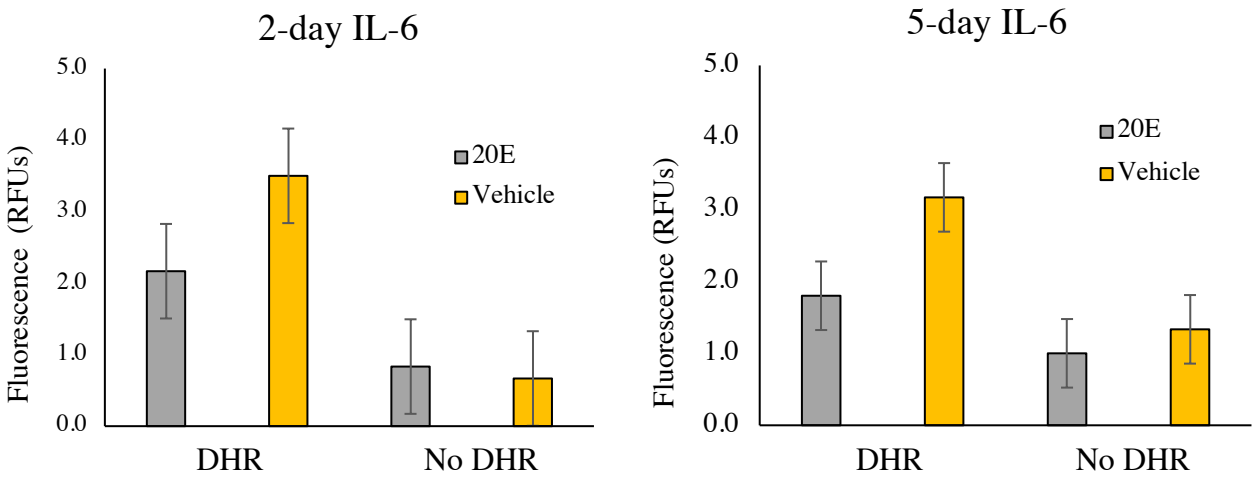

Figure 6. Expression of IL-6 Determined by Observed Fluorescence Analysis
Expression of IL-6, quantified in terms of average fluorescence (in RFUs), where 0 = no fluorescence and 5 = most fluorescence, is shown on the y-axis. On the x-axis is treatment groups, arranged by injury (DHR vs. No DHR), with yellow bars representing Vehicle treatment and gray bars representing 20E. Error bars for both graphs reflect standard error.

For the semi-quantitative ImageJ analysis, fluorescence intensity was corrected for background signal and reported as CTF. This method produced results with trends nearly identical to those from the observed fluorescence results for MCP-1 in 2-day treatment groups. In the 5-day DHR groups, ImageJ analysis showed vehicle treated mice having less fluorescence than 20E treated, this was not supported by the observed fluorescence analysis, as it reflected the opposite relationship. This method also supports the observed fluorescence analysis for IL-6 at both the 2-day and 5-day timepoints, since similar relationships were observed between treatment groups. Average CTF values for each treatment group are shown below in Figure 7.

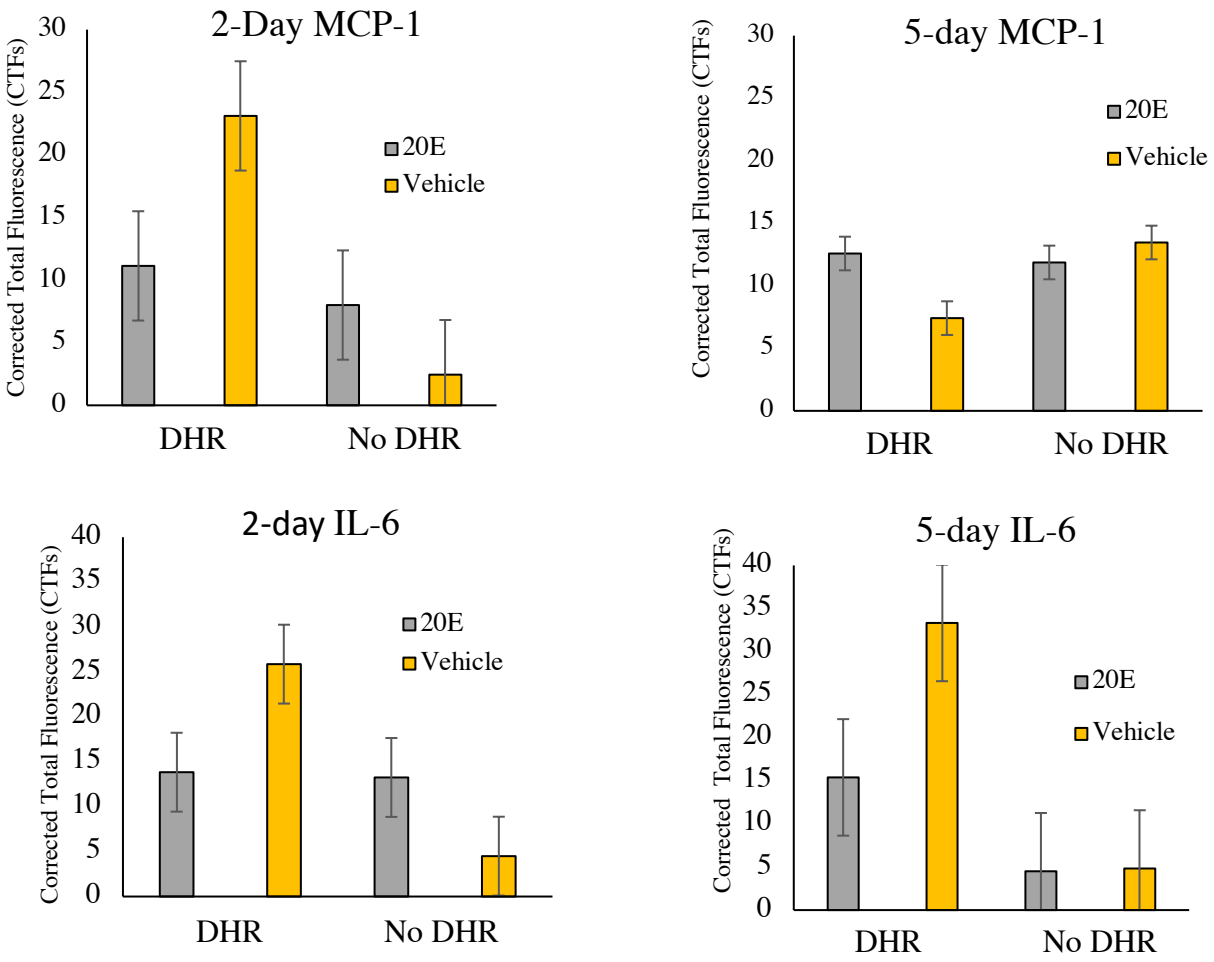

Figure 7. Expression of MCP-1 and IL-6, Determined by ImageJ Analysis

Expression of the respective cytokine (denoted above each graph) is shown on the y-axis as corrected total fluorescence (CTF), in arbitrary units of CTF. On the x-axis is treatment groups, arranged based on injury (DHR vs. No DHR), with yellow bars represent Vehicle treatment, while gray bars represent 20E, with error bars for both groups corresponding to respective standard deviations

DISCUSSION

The aim of this study was to determine if phytoecdysteroid supplementation affects the expression of inflammatory cytokines, IL-6 and MCP-1, in skeletal muscle of young mice after an acute bout of downhill running. Tissue wet mass to body mass ratios for each group determined that there was no significant differences between various treatment groups. No drastic changes in tissue weight or body mass were observed either. Abnormal weight loss has been shown to be an indicator of poor health or stress in animals; knowing this, the normalized mass ratios indicate that mice were healthy across all groups. (Folts, et al., 1999) For all DHR groups, the normalized tissue wet mass to body weight ratio was found to be slightly lower than the similarly treated No DHR groups. While statistically insignificant, the difference between DHR and No DHR groups could be physiologically relevant, a result of possible phagocytic activity removing damaged material from the muscle.

From analysis of the H&E stained sections, discreet areas of distorted fiber structure and extra nuclei present were observed for the DHR groups, indicating that the acute bout of DHR to exhaustion did result in injury. (Tsivitse, et al., 2009) The occurrence of injury was further supported by the immunohistochemical (IHC) identification of IL-6. For IL-6, more fluorescence was seen in the DHR than No DHR groups, which indicates a greater expression/abundance of IL-6. Since IL-6 expression has been shown to increase at a rate related to the magnitude of damage, the increased IL-6 shows that the acute bout of DHR successfully resulted in injury. (Bruunsgard, et al., 1997) Expression of MCP-1, quantified in terms of fluorescence, was also found to be higher in DHR than No DHR groups, indicating that injury occurred since this signaling cytokine is specific to macrophages, which account for an important part of the tissue repair process.

While the acute bout of DHR did produce some areas of deformed fiber structure in the muscle, the magnitude of damage was low; the damaged areas were infrequent and small in respect to the total cross-sectional size of the gastrocnemius muscle. No overall morphological trends were seen between treatment groups, previous studies have shown this as well (Tsivitse, et al., 2003) The additional nuclei observed at sites of damage in the H&E stained sections likely corresponded to monocytes, such as neutrophils and macrophages, as they infiltrated the tissue to obliterate and repair the damaged muscle (Tidball, 1995). To confirm this, IHC identification of these cell types would have been necessary. It was initially planned to separately identify neutrophils, M1, and M2 macrophages; however issues with reactivity/specificity of the appropriate antibodies prevented this from happening.

Semi-quantitative analysis of inflammatory cytokines revealed some interesting findings. Following DHR, 2 days of treatment with 20E appeared to result in less IL-6 fluorescence than vehicle treatment, indicating possible lower levels of IL-6 expression with 20E treatment. After 5 days of treatment, the difference in IL-6 expression between the two treatments remained similar, since the observed fluorescence had been reduced by a similar magnitude in both. The reduction in IL-6 expression suggests that 20E may exhibit anti-inflammatory activity in response to eccentric skeletal muscle damage.

Treatment of 20E for 2 days after DHR was observed to result in less fluorescence of MCP-1 specific antibodies than vehicle treatment. A similar, although weaker, trend was seen with 5 days of treatment. This indicates that 20E may have reduced, or more specifically, suppressed the increase in MCP-1 expression following eccentric damage. Reduction of this cytokine, responsible for the signaling of macrophage infiltration, further supports that 20E treatment after DHR may exhibit anti-inflammatory activity. The ImageJ results generally supported these results from the semi-quantitative analysis of observed fluorescence, however

with the variability in fluorescence between samples, small sample size, and frequent artifacts, the definitive values from ImageJ are likely no more precise than the analysis of observed fluorescence. Because of this, the ImageJ data only functioned as supplemental.

Specifically among the No DHR groups, there was a large amount of variability between samples. Since there was no possible source of injury to differ in magnitude, the variability can likely be attributed to the IHC procedure and the slides tissue sections were mounted out. Since no fixation steps were used in this IHC protocol to secure tissues to the slide, electrostatic interactions between negatively charged components of the tissue (such as ions, proteins, or genetic material), and a positively charged microscope slide, were solely responsible for keeping the tissue section adhered. Roughly 70% of the samples were mounted to uncharged slides, which frequently resulted in tissue sections floating up off the slide during wash steps. Extreme caution was used during IHC staining, yet many sections moved around throughout this process, resulting in wrinkles and/or folds.

While these results are congruent with the previous literature that had shown 20E to have anti-inflammatory abilities, these findings are contrary to my original hypotheses. Numerous studies have shown 20E to exhibit effects such as increasing protein synthesis and rodent grip strength, both of which are similar to the effects of anabolic steroids. Anabolic steroids increase inflammation in response to damage in skeletal muscle, which is the exact opposite of what was observed with the treatment of 20E in this study. The reduced inflammation with 20E treatment is more akin to the behavior of catabolic, rather than anabolic steroids.

The exact pathway or mechanism that renders 20E a biologically active compound in skeletal muscle of mammals is unknown, though it is believed to bind to a cell surface membrane bound G-protein coupled receptor. I propose that a novel mechanism may exist, which is responsible for regulating a switch between the catabolic and anabolic activity of 20E. Inhibition

or activation of the Notch signaling pathway has been shown to play a role in altering the expression of MCP-1 and IL-6 during an inflammatory response (Arthur, et al., 2014). The pathway between Notch signaling and cytokine expression is currently unknown, although some work has shown it may involve a nuclear factor kappa-light-chain-enhancer of activated B cells (NF-κB) mechanism (Hindi, et al., 2012). Additionally, previous work in the Zwetsloot lab has found that 20E reduced protein synthesis in skeletal muscle after an acute bout of DHR to exhaustion, which further supports a novel switch mechanism to allow catabolic-steroid like behavior of 20E in response to skeletal muscle damage (unpublished data).

Like all systems within the body, there is a fine balance in the repair of skeletal muscle injuries between too little of an inflammatory response, which does allow complete and timely recovery, and too much, which can result in additional damage and eventually lead to disease. The current study demonstrates that 20E may have an anti-inflammatory effect in response to an acute, eccentrically damaging event in skeletal muscle. It is possible that 20E may be useful in combating diseases such as sarcopenia, where the inflammatory capacity is altered leading to progressive loss of muscle mass (Peake, et al., 2010). Future work should strive to elucidate the mechanism responsible for biological activity of 20E. The Notch-mediated regulation of inflammatory cytokines such as MCP-1 and IL-6 in response to skeletal muscle damage also warrants further investigation.

REFRENCES

Arthur, S., Zwetsloot, K., Lawrence, M., Nieman, D., Lila, M., Grace, M., . . . Greiner, R. (2014). Ajuga turkestanica increases Notch and Wnt signaling in aged skeletal muscle. *Eur Rev Pharmacol Sci, 18*(17), 2584-2592.

Beiner, J., Jokl, P., & Panjabi, M. (1999). The effect of anabolic steroids and corticosteroids on healing of muscle contusion injury. *Am J Sports Med, 27*(1), 2-9.

Bruunsgard, H., Galbo, H., halkjaer-Kristensen, J., Johansen, T., Maclean, D., & Pedersen, B. (1997). Exercise-induced increase in serum interleukin-6 in humans is related to muscle damage. *J Physiol, 499*(15), 833-841.

Douglas, M., Pearson, S., Ross, A., & McGuigan, M. (2017). Eccentric Exercise:Physiological characteristics and acute responses. *Sports Med, 47*(4), 663-675.

Folts, J., & Ullman-Cullere, M. (1999). Guidlines for assessing the health and condition of mice. *28*(4), 28-32.

Gorelick-Feldman, J., Cohick, W., & Raskin, I. (2010). Ecdysteroids elict a rapid Ca2+ flux leading to AKt activiation and increased protein synthesis in skeletal muscle cells. . *Steroids, 75*(10), 632-637.

Gorelick-Feldman, J., Maclean, D., Illic, N., Poulev, A., Lila, M., Cheng, D., & Raskin, I. (2008). Phytoecdyersoids increase protein synthesis in skeletal muscle cells. *J Agric Food Chem, 56*(10), 3532-3537.

Hindi, S., Paul, P., Dahiya, S., Mishra, V., Bhatnagar, S., Kuang, S., . . . Kumar, A. (2012). Reciprocal interaction between TRAF6 and notch signaling regulates adult myofiber regeneration upon injury. . *Mol Cell Biol, 32*(23), 4833-4845.

Hody, S., Lacrosse, Z., Leprince, P., Collodoro, M., Croisier, J., & Rogister, B. (2013). Effects of eccentrically and concentrically biased training on mouse muscle phenotype. *Med Sci Sports Exerc, 45*(8), 1460-1468.

Kurmukov, A., & Syrov, V. (1988). Anti-inflammatory properties of ecdysterone . *Medicinal'nii Zhurnal Uzbekistana, 10*, 68-70.

Labno, C. (n.d.). *Basic quantification of intensity with ImageJ*. (Integrated Light Microscopy Core, University of Chicago) Retrieved April 22, 2018, from www.unige.ch

Lafont, R., & Dinan, L. (2003). Practical uses for ecdysteroids in mammals including humans: an update . *J Insect Sci, 3*(7).

Liping, Z., Ran, L., Garcia, G., Wang, X., Han, S., Jie, D., & Mitch, W. (2009). Chemokine CXCL16 regulates nreutrophil and macrophage infiltration into injuried muscl, promoting muscle regeneration. *Musculo Path, 175*(6), 2518-2527.

Marqueste, T., Giannesini, B., Fur, Y., & Cozzone, P. (2008). Comparative MRI analysis of T2 changes associated with single and acute bouts of downhill running teading to eccentric-induced muscle damage. *J Appl Physiol, 105*(1), 299-307.

Munoz-Canoves, P., Scheele, C., Pedersen, B., & Serrano, A. (2013). Interleukin-6 myokine signaling in skeletal muscle: a double-edged sword? *FEBS, 280*(17), 4131-4148.

Nielsen, A., & Pedersen, B. (2007). The biological roles of exercise-induced cytokines: IL-6, IL-8 and IL-15. *32*, 833-839.

Peake, J., Della Gatta, P., & Cameron-Smith, D. (2010). Aging and its effects on inflammation in skeletal muscle at rest and following exercise-induced muscle injury. *Am J Physiol Regul Integr Comp Physiol, 298*(6), 1485-1495.

Pierre-Schneider, B., & Tiidus, P. (2007). Neutrophil infiltration in exercise-injured skeletal muscle. *Sports Med, 37*(10), 837-856.

Reid, M., Shoji, T., Moody, M., & Entman, M. (1992). Reacive oxygen in skeletal muscle. II Extracellular release of free radicals. *J Appl Physiol, 73*, 1392-1397.

Serrano, A., Baeza-Reja, B., Perdiguero, E., Jardi, M., & Munoz-Canoves, P. (2008). Interleukin-6 is an essential regulator of satellite cell mediated skeletal muscle hypertrophy. *Cell Metab, 1*, 33-44.

Tidball, J. (1995). Inflammatory cell response to acute muscle injury. *Med & Sci in Sports & Exerc, 27*(7), 1022-1032.

Tidball, J. (2005). Inflammatory processes in muscle injury and repair. *Am J Physiol Regul Integr Comp Physiol*(288), 345-353.

Tidball, J., & Vilalta, A. (2010). Regulatory interactions between muscle and the immune system during muscle regeneration. *J. Physiol Integr Comp Physiol, 298*, 1173-1187.

Tidball, J., & Wehling-Henricks, M. (2007). Macrophages promote muscle membrane repair and muscle fibre growth and regeneration during modified muscle loading in vivo. *J Physiol, 578*, 327-336.

Tsivitse, S., McLoughlin, T., Peterson, J., Mylona, E., McGregor, S., & Pizza, F. (2003). Downhill running in rats: influence on neutrophils, macrophages, and MyoD+ cells in skeletal muscle. . *Eur J Appl Physiol , 90*(5-6), 633-638.

Tsivitse, S., Peters, M., Stoy, A., Mundy, J., & Bowen, R. (2009). The effect of downhill running on Notch signaling in regenerating skeletal muscle. *Eur J Appl Physiol, 106*(5), 759-767.

Vita

William Luke Johnson IV was born in Greensboro, NC to Pam and Bill Johnson. He graduated from Bishop McGuinness Catholic High School in Kernersville, North Carolina, in 2014. The following fall he was admitted to Appalachian State University in Boone, NC. William is currently pursuing a B.S. in Chemistry with University Honors at Appalachian State University, and is projected to graduate in May 2018.